Real-time Electric Field Estimation for HVDC Cable Dielectrics

Z. Y. Huang*, J. A. Pilgrim, P. L. Lewin and S. G. Swingler
Tony Davies High Voltage Laboratory
University of Southampton
Southampton, United Kingdom
*zh2g09@soton.ac.uk

***Abstract* — For HVDC cables, dielectric field inversion normally occurs due to the temperature drop across the insulation. Unlike AC applications where the field distribution is primarily determined by the cable geometry, the DC field can be significantly affected by the load current and hence the dielectric temperature profile. Higher temperature drops lead to higher electrical stress at the insulation screen, increasing the risk of breakdown. Thus, a real-time dielectric DC field estimator would be very useful to prevent over-stressing the cable. Theoretically, the electrical field can be calculated from the overall dielectric temperature drop. Therefore, by monitoring the temperature profile and integrating with mathematical algorithms, the DC field distribution might be assessed in real time. In this paper, a mathematical algorithm for calculation of the DC field is demonstrated, using standard online temperature monitoring techniques.**

Keywords — condition monitoring; electric breakdown; power cable insulation

I. INTRODUCTION

For high voltage power cable transmission, it is critical to prevent the dielectric being overstressed, potentially leading to increased risk of electrical breakdowns in the long term. Under AC operating voltage, the dielectric field distribution is capacitively graded and mainly determined by the cable geometry. During operation, the highest stress is found close to the conductor screen and keeps constant as long as the operating voltage does not change [1]. In other words, dielectric breakdown due to overstressing is unlikely to occur throughout the whole asset life if a cable design passes the initial routine and type tests.

Conversely, for modern HVDC applications, the dielectric field becomes resistively graded due to the non-zero dielectric leakage current. The electrical resistivity, ρ_r, is described as an empirical exponential function of local temperature and electrical stress, for both continuous and transient analysis [2]:

$$\rho_r = \rho_0 \exp(-\alpha\theta_r)\exp(-\gamma E_r) \quad (1)$$

Where; ρ_0 is the reference electrical resistivity at 0°C and 0kV.mm^{-1} (Ω.m^{-1}), α the temperature dependency coefficient (°C^{-1}), γ the electrical field dependency coefficient (mm.kV^{-1}), θ_r the temperature at radius r (°C), and E_r is the electrical stress at radius r (kV.mm^{-1}). As a result, the so called 'field inversion' occurs with the highest stress being close to the insulation screen and heavily affected by the temperature drop across the insulation. According to [3], the DC dielectric field can be numerically calculated by:

$$E_r = \frac{U r^{k-1} e^{-\gamma E_r}}{\int_{R_i}^{R_o} r^{k-1} e^{-\gamma E_r} dr} \quad (2)$$

$$k = \frac{\alpha\theta_{drop}}{\ln R_o - \ln R_i} \quad (3)$$

Where; E_r is the local electrical stress at radius r (kV.mm^{-1}), U the applied voltage across the insulation (kV), R_i the inner radius of the insulation (mm), R_o the outer radius of the insulation (mm), and θ_{drop} is the temperature drop across the insulation (K). In Fig. 1 below, the dielectric field distribution is plotted under various temperature drops, showing the change in stress profile with temperature.

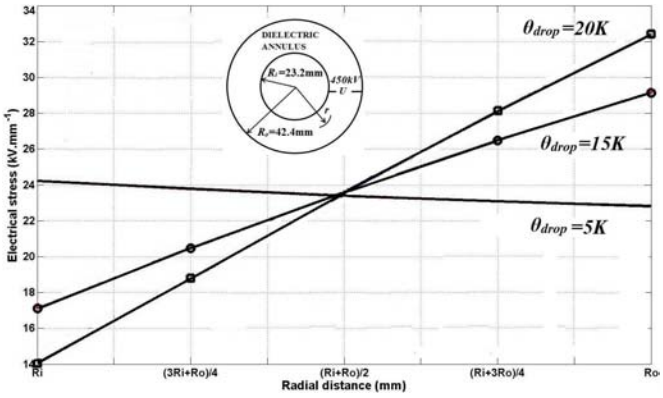

Fig. 1. Illustration of dielectric field inversion

As the maximum dielectric stress is shown to be uniquely linked with the dielectric temperature drop in Fig. 1, the maximum allowable temperature drop is often specified by cable manufacturers, determined with reference to the maximum dielectric breakdown strength. One feature proposed in this work is to assess the real-time stress distribution through online dielectric θ_{drop} monitoring.

II. CONDITION MONITORING APPLICATION

In this chapter, mathematical algorithms are developed for the dielectric θ_{drop} to be evaluated in real time, using existing cable thermal condition monitoring technique. Two key motivations for this are:

1. As the ambient thermal environment (e.g. backfill drying condition, ground surface temperature) may change during transient operation, the traditional theoretical transient thermal model may not be accurate enough unless relevant environmental parameters are updated.
2. Practical HV cables are expected to be able to operate safely for some time under an overstressed condition [4], which interests researchers to find out how long this 'safety' would last and what the affecting factors are.

Therefore, the real-time dielectric θ_{drop} monitoring can be very useful to answer above questions because it is closely linked to the dielectric electrical stress state.

At present, the cable surface temperature can be effectively monitored via distributed temperature sensing (DTS) devices [5]. However, it is still challenging to measure any inner cable layer temperature due to the difficulties of installing the fibre. Although Cigré has proposed mathematical models for the transient temperature calculation [6], it is numerical and the accuracy can be largely affected by the backfill thermal resistivity, requiring frequent measurements in an ideal case. Therefore, an analytical transient model combining the above two approaches is proposed, which calculates the dielectric $\theta_{drop}(t)$ as a function of cable loading $I(t)$ and cable surface temperature $\theta_e(t)$. As the primary benefit, all the thermal changes in ambient environment can be equivalently represented by the cable surface temperature variation which is monitored by DTS in real time.

Under the steady state in Fig. 1, the dielectric stress distribution is shown as a function of dielectric θ_{drop}. If this also applies to transient, the insulation can be simplified into one single layer. Otherwise, subdivision and the Cigré calculation [6] are required to obtain the local temperature. To verify this, a practical monopole cable design is tested under a 24-hour step load transient (i.e. 2000A applied at t = 0s), with the initial cable temperature the same as ambient. Note that 2000A is limited by a maximum steady-state dielectric strength of 30kV.mm^{-1} for MI cables [7], which leads to a dielectric θ_{drop} of around 13°C. This is considered appropriate because scheduled load transients can be analysed as the superposition of several fundamental step loads [1]. Modelling parameters are summarised in Table I and FEA simulation results for electrical and thermal fields are plotted in Fig. 2, using the method in [7].

TABLE I. MODELLING PARAMETERS SUMMARY

(Cu) conductor outer diameter	60.5	mm
conductor cross-section area	2500	mm^2
maximum conductor design temperature	50	°C
conductor volumetric heat capacity	3.45×10^6	J.m^{-3}.K^{-1}
conductor thermal resistivity	0.0026	K.m.W^{-1}
(MI-paper) insulation outer diameter	101	mm
insulation volumetric heat capacity	2×10^6	J.m^{-3}.K^{-1}
insulation thermal resistivity	6	K.m.W^{-1}
(Pb) sheath outer diameter	111	mm
sheath volumetric heat capacity	1.45×10^6	J.m^{-3}.K^{-1}
sheath thermal resistivity	0.02833	K.m.W^{-1}
(PE) serving outer diameter	120	mm
serving volumetric heat capacity	2.4×10^6	J.m^{-3}.K^{-1}
serving thermal resistivity	3.5	K.m.W^{-1}
backfill specific heat capacity	2.1×10^6	J.kg^{-1}.K^{-1}
backfill thermal resistivity	1.2	K.m.W^{-1}
ambient temperature	12	°C
nominal voltage	500	kV
burial depth	2	m

In Fig. 2, both fields evolve simultaneously and the overall dielectric stress distribution under transient shows a similar profile to Fig. 1. This implies that θ_{drop} can be used as an indicator of the transient stress field evolution. More importantly, the results imply that the insulation layer can be simply modelled by a pair of equivalent lumped quantities, i.e. thermal resistance and capacitance, without any subdivisions.

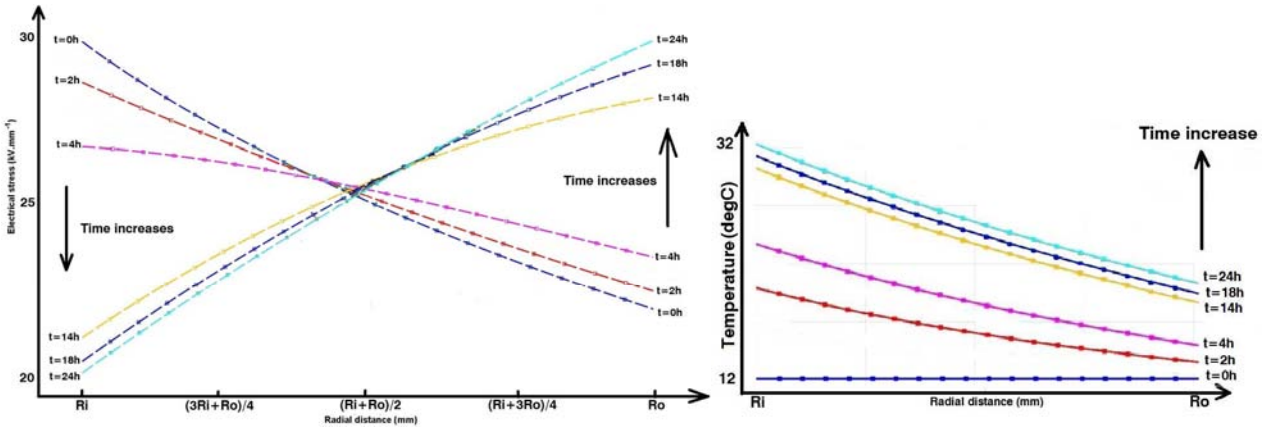

Fig. 2. Dielectric electrical and thermal field evolution under a 24-hour step transient

Fig. 3 below shows a simplified transient thermal network analogy.

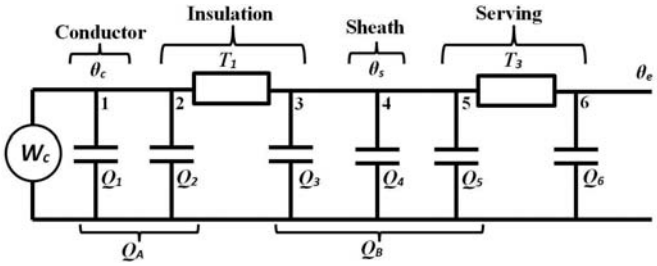

Fig. 3. Equivalent transient thermal network

In Fig. 3, the metallic conductor and sheath are modelled by their lumped thermal capacitances, Q_1 and Q_2, with negligible thermal resistance. The non-metallic insulation and serving are modelled by by the 'π' shape thermal capacitance-resistance-combination, which was initially proposed by Van Wormer [8] and later adopted by IEC60853 [9]. Note that other cable structures such as oil-filled, armoured, etc., can be represented as the standard two-loop network equivalent ($Q_A = Q_1 + Q_2$ and $Q_B = Q_3 + Q_4 + Q_5$) shown in Fig. 3, through the method outlined in IEC60853.

To calculate the transient dielectric $\theta_{drop}(t)$ as a function of time-variant $\theta_e(t)$ and current loading $I(t)$, the following conditions are assumed.

- Cable system was in thermal steady state (either loaded or off loaded) before the transient starts at $t = t_0$.
- Dielectric leakage current loss is assumed negligible [10]. Note that it won't affect the field inversion because the dielectric θ_{drop} is mainly caused by the much greater joule loss [7].
- The conductor loss is modelled by a step function at $t = t_0$. For variable excitation (e.g. square), the overall response is the superposition of the responses due to each single step [11].

According to the energy conservation law, simultaneous equations are drawn for nodes 2 and 4 as follows, over a small time interval between t and $t+\Delta t$.

$$\frac{Q_1+Q_2}{\Delta t}\left[\theta_c(t+\Delta t)-\theta_c(t)\right]=W_c-\frac{\theta_c(t+\Delta t)-\theta_s(t+\Delta t)}{T_1} \tag{4}$$

$$\frac{Q_3+Q_4+Q_5}{\Delta t}\left[\theta_s(t+\Delta t)-\theta_s(t)\right]=\frac{\theta_c(t+\Delta t)-\theta_s(t+\Delta t)}{T_1}-\frac{\theta_s(t+\Delta t)-\theta_e(t+\Delta t)}{T_3} \tag{5}$$

Where; W_c and $\theta_e(t+\Delta t)$ are boundary conditions, and $\theta_c(t)$ and $\theta_s(t)$ are initial conditions. Therefore, by solving equations (4) and (5) for $\theta_c(t+\Delta t)$ and $\theta_s(t+\Delta t)$, the target parameter $\theta_{drop}(t+\Delta t)$ can be calculated through equation (6) to (9).

To integrate the mathematical equations into the existing thermal condition monitoring system, the following algorithm is proposed.

Step 1. Suppose a transient step load starts at time $t = t_0$ with initial conditions $\theta_c(t_0)$ and $\theta_s(t_0)$ (e.g. calculated through IEC60287).

Step 2. Specify the time interval Δt and measure the surface temperature $\theta_e(t_1)$ through DTS system at time $t_1=t_0+\Delta t$. By substituting the above parameters into equation (6) to (9), $\theta_c(t_1)$, $\theta_s(t_1)$ and $\theta_{drop}(t_1)$ are calculated.

Step 3. For the next step at $t_2=t_1+\Delta t$, $\theta_c(t_1)$ and $\theta_s(t_1)$ become the initial conditions and the surface temperature $\theta_e(t_2)$ is re-measured.

Step 4. Iteratively, the transient dielectric $\theta_{drop}(t)$ can be monitored at $t_1, t_2, t_3, t_4, \ldots, t_n$.

As an illustration, the previous test in Fig. 2 is repeated with the relevant temperature evolutions being calculated and plotted in Fig. 4. Note that the real-time $\theta_e(t)$ data is exported from the FEA model and used in equations (6) to (8).

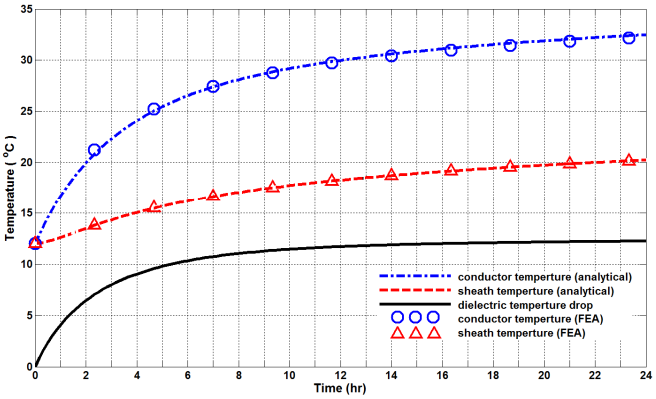

Fig. 4. Temperature evolution over a 24-hour step load transient

In Fig. 4, it is shown that the developed analytical temperature cable temperature agrees well with the numerical FEA modelling within a difference less than 2°C, and the dielectric θ_{drop} gradually increases towards 13°C.

$$\theta_c(t+\Delta t)=\frac{\left[\Delta t\cdot W_c+(Q_1+Q_2)\cdot\theta_c(t)\right]\cdot\left[\Delta t(T_1+T_3)+T_1T_3(Q_3+Q_4+Q_5)\right]+\Delta tT_3(Q_3+Q_4+Q_5)\cdot\theta_s(t)+\Delta t^2\theta_e(t+\Delta t)}{\Delta tT_3(Q_1+Q_2)+\left[T_3(Q_3+Q_4+Q_5)+\Delta t\right]\cdot\left[T_1(Q_1+Q_2)+\Delta t\right]} \tag{6}$$

$$\theta_s(t+\Delta t)=\frac{T_3\left[\Delta t^2\cdot W_c+\Delta t(Q_1+Q_2)\cdot\theta_c(t)\right]+\left[T_1(Q_1+Q_2)+\Delta t\right]\cdot\left[T_3(Q_3+Q_4+Q_5)\cdot\theta_s(t)+\Delta t\cdot\theta_e(t+\Delta t)\right]}{\Delta tT_3(Q_1+Q_2)+\left[T_3(Q_3+Q_4+Q_5)+\Delta t\right]\cdot\left[T_1(Q_1+Q_2)+\Delta t\right]} \tag{7}$$

$$\theta_{drop}(t+\Delta t)=\theta_c(t+\Delta t)-\theta_s(t+\Delta t)=\frac{\left[T_1T_3(Q_3+Q_4+Q_5)+\Delta tT_1\right]\cdot\left[\Delta t\cdot W_c+(Q_1+Q_2)\cdot\theta_c(t)\right]-T_1(Q_1+Q_2)\cdot\left[T_3(Q_3+Q_4+Q_5)\cdot\theta_s(t)+\Delta t\cdot\theta_e(t+\Delta t)\right]}{\Delta tT_3(Q_1+Q_2)+\left[T_3(Q_3+Q_4+Q_5)+\Delta t\right]\cdot\left[T_1(Q_1+Q_2)+\Delta t\right]} \tag{8}$$

$$W_c=I^2R_{dc}\cdot\left\{1+\alpha_{20}\cdot\left[\theta_c(t)-20\right]\right\} \tag{9}$$

Theoretically, the thermal field evolution is expected to lead that of the electric field, due to a time delay spent on space charge relocation (i.e. trapping, de-trapping [12]). In other words, there can be a transient 'safety' period when the cable is implied electrically overstressed (based on θ_{drop}). To study this 'safety' period, several tests are designed with the current loading varying from 1000A (i.e. half the nominal value) to 4000A (i.e. double the nominal value). In Table II below, the time required to reach θ_{drop}=13°C and 30kV.mm^{-1} at the insulation screen are recorded separately for a comparison.

TABLE II. STUDY OF THE 'SAFETY' TRANSIENT

Preload (A)	Transient load (A)	Time to θ_{drop}=13°C (min)	Time to $E(R_o)$ =30kV.mm^{-1} (min)	Time delay (hr)
1000	2500	133	295	2.7
1000	3000	63	181	2.0
1000	4000	26	110	1.4
1250	2500	111	240	2.2
1250	3000	52	148	1.6
1250	4000	21	84	1.1
1500	2500	82	178	1.6
1500	3000	38	109	1.2
1500	4000	15	62	0.8
1750	2500	46	106	1.0
1750	3000	20	66	0.8
1750	4000	8	40	0.5

In Table II, it is firstly confirmed that the thermal field evolution is always leading the corresponding electrical field evolution. Under this test, the time delay, i.e. safety period, varies from 0.5 to 2.7 hours. Secondly, a lower preload generally requires a longer time to reach the dielectric breakdown stress and also has a longer time delay. This is because, during the transient, it takes more time for the dielectric as a thermal capacitance to reach its temperature drop limit with a lower initial temperature (i.e. lower preload) than with a higher starting temperature (i.e. higher preload). It means that more time is required to achieve a certain thermal energy level, motivate the space charge relocation, and build up the resulting electrical field. However, this charging process (i.e. energy transfer from thermal to electrical) can be shortened by a higher transient load because more energy will be pumped into the system per unit time. Effectively, it accelerates the space charge relocation process, i.e. equation (1), and therefore reduces the time delay between the thermal and electrical field evolutions.

III. CONCLUSIONS

This paper has presented the application of existing thermal monitoring systems to assess the dielectric electrical stress conditions of HVDC cables. As an initial approach, this work briefly introduces the logic, derives the fundamental mathematics and presents some sample calculations. Valuable information verifies the existence of the 'safety period' and further indicates that although the safety period varies from case to case, for cable specifications similar to the one under test, it is more likely to be less than 3 hours because the above test covers the most typical loading range in transient operations. However, further work is suggested to study and quantify the time constant of space charge relocation so that the transient stress distribution might be directly calculated as a function of cable loading and DTS readings.

REFERENCES

[1] G. F. Moore, *Electric Cables (HANDBOOK)*, Wiley-Blackwell Press, 1997.

[2] T. Worzyk, Submarine Power Cables: Design, Installation, Repair, Environmental Aspects, Springer, 2009.

[3] M. Jeroense, Charges and Discharges in HVDC Cables: In Particular in Mass-impregnated HVDC Cables, Delft: Delft University Press, 1997.

[4] Cigré Working Group 02-Study Committee 21, Recommendations for tests of power transmission dc cables for a rated voltage up to 800kv, Electra(189), 2000.

[5] H. J. Li, K. C. Tan and Qi Su, "Assessment of underground cable ratings based on distributed temperature sensing," *IEEE Trans. Power Delivery,* vol. 21(4), pp. 1763-1769, 2006.

[6] Cigré Working Group 02-Study Committee 21, Computer method for the calculation of the response of single-core cables to a step function thermal Transient, vol. 87, Electra, 1983, pp. 41-64.

[7] Z. Y. Huang, J. A. Pilgrim, P. L. Lewin, S. G. Swingler and D. Payne, "Current rating methodology for mass impregnated HVDC cables," *IEEE 2013 Electrical Insulation Conference*, Ottawa, Jun, 2013.

[8] V. Wormer, "An improved approximate technique for calculating cable temperature transients," *Tans. Amer. Inst. Elect. Eng*, vol. 74, part 3, pp. 277-280, 1955.

[9] Calculation of the cyclic and emergency current rating of cables, Part2: Cyclic rating of cables greater than 18/30 (36) kV and emergency rating s for cables of all voltages, CEI IEC 60853-2, 1989.

[10] Electric cables – Calculation of the current rating – Current rating equation (100% load factor) and calculation of losses – General, BS IEC 60287-1-1, 2006.

[11] G. J. Anders, Rating of Electric Power Cables: Ampacity Computations for Transmission, Distribution and Industrial Applications, McFRAW-HILL, 1997.

[12] P. Morshuis, M. Jeroense, "Space charge measurements on impregnated paper: a review of the PEA method and a discussion of results," *IEEE Electrical Insulation Magazine*, vol.13(3), 1997, pp. 26-35.